Calibration of the Performance Measurement for Thin Vapor Chambers by Photonics Technologies

Kuang-Yu Hsu, Yi-Jing Chu, Andhi Indira Kusuma, Krishn Patel, Rajveer G. V., and Ming-Hsien Hsiao
T-Global Technology Co.
No. 33, Ln. 50, Daren Rd., Taoyuan Dist., Taoyuan City, Taiwan
kyhsu@tglobalcorp.com

Abstract

Characterization of thin vapor chambers is performed using laser heating and non-contact infra-red pyrometers for temperature measurement. This is found to be a fast and accurate measurement for mass production applications. The temperature measurement at the heater position on the evaporator side is very critical but it is seriously affected by the heat laser light. For accuracy considerations the measurement requires a pulsed heating mode to allow the measurement to be made while the laser is off. The heater operates in an on-off heating mode rather than a continuous heating mode. It is necessary to analyze the deviation from the continuous heating mode. Two methods, including matching the heat and matching the temperature, are proposed and experimentally measured. The temperature accuracy of the on-off laser heating is less than ±1 °C. The measurement data also show the transient response of the vapor chamber to a heat surge is temperature stabilizing. In this study the effective heat capacity is proposed and used for the assessment of temperature stabilization performance. The experimental data also show the effective thermal capacity of the vapor chamber is 2.5 times larger than that of the copper plate.

Keywords

Thin vapor chamber, vapor chamber characterization, vapor chamber transient analysis

1. Introduction

Traditionally, graphite sheets with a high thermal conductivity in the transverse direction have been used as the heat spreaders. The vapor chamber (VC), utilizing the two-phase mechanism rather than material thermal conduction, is an even more effective heat spreader. The thin VC, with the thickness less than 1.0 mm, has the potential for relieving the thermal issues in portable device applications with limited available space. The working range of the heating power of the thin VCs is usually less than 10 W, limited by the amount of the working fluid. The performance characterization of the thin VCs, using the contact heater and the thermocouples, suffers from the large thermal capacity as well as the large heat loss of the metal conductor to deliver the heat to the device under test [1]. The measurement time usually takes several minutes and the heat loss is yet to be improved. A laser heater needs no metal conductor to deliver the heat current [2], but the temperature measurement, using the infra-red pyrometer at the heater position on the evaporator side, is seriously affected by the scattered and reflected heat laser light. To take the temperature with accuracy, the output beam of the heating laser is shut off for a short period of time [3]. The laser heating is much more effective with much smaller heat loss than the contact heating so a measurement time of only 60 seconds is good enough. However, the off time in the on-off heating scheme introduces a deviation in the system from the continuous heating. In this study, two calibration methods of the on-off laser heating scheme by matching the heat and by matching the temperature are proposed and experimentally demonstrated. A good temperature stabilizing performance of the vapor chamber is also found from the transient response data during the 50-ms laser off time. The effective thermal capacity parameter is proposed and used for the assessment of temperature stabilization performance.

2. Measurement System

The setup of the measurement system is shown in Fig. 1. An 808-nm infra-red (IR) laser with a collimated output from the multi-mode fiber is used as the heating source. The non-contact temperature measurement is done using the IR thermometers or pyrometers (CTlaser 4ML, optris). The thermal radiation from an object is related to its emissivity and its temperature. The emissivity is dependent on the material and also wavelength dependent. A pyrometer receives the thermal radiation in the infra-red range from the object at a distance through a suitable optical lens. By careful calibration with the emissivity of the object, the received signal is converted to the temperature. Conventionally, a thermopile detector has been used in the pyrometer, but the response speed is quite slow. Recently, much faster photodiodes have been developed and adopted in the pyrometers, facilitating millisecond level temperature measurement. The heating and temperature measurement in this system are both non-contact.

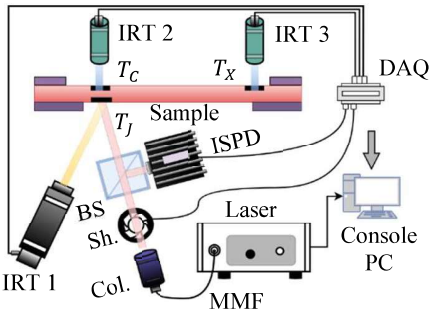

Fig. 1. Schematic system set-up. IRT: infra-red thermometer. BS: beam splitter. ISPD: integrated sphere with a photodiode detector. Sh.: shutter. Col.: collimator. MMF: multi-mode fiber.

The temperatures, T_J on the evaporator side and T_C and T_X on the condenser side of the sample, are measured. The temperatures T_C and T_X, at positions with a separation of 50 mm, are for the temperature uniformity. The position of T_J is in contact with the heat source, i.e., the chip. The non-contact measurement of T_J using a pyrometer is seriously affected by the scattered 808-nm laser light. To reduce the interference, the laser output beam is periodically shut off for a short period of

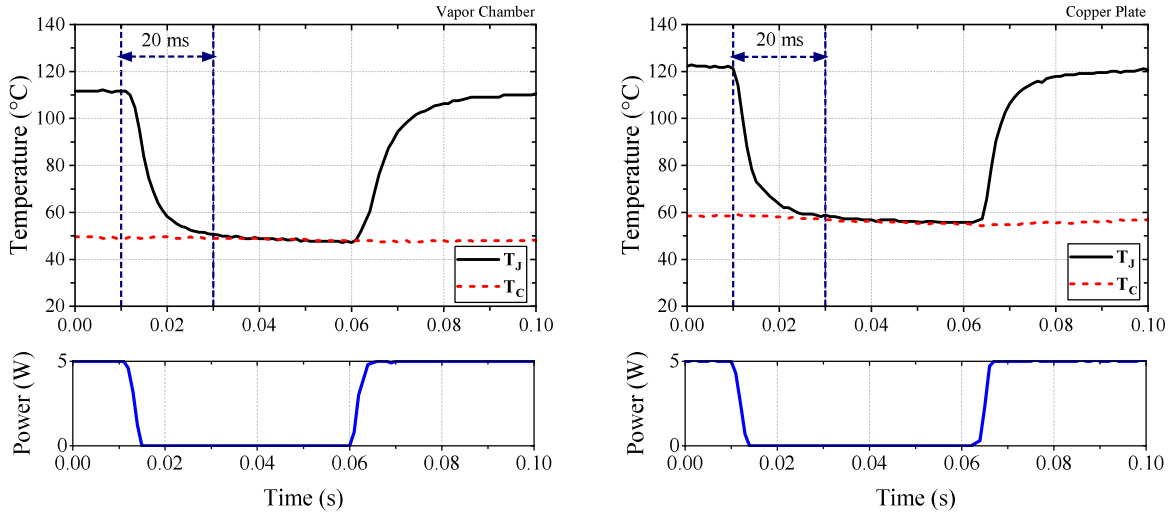

Fig. 2. The original T_J, T_C, and the heat current curves of (a) the VC and (b) the copper plate.

time using a mechanical shutter (SH05R, Thorlabs) with a high optical isolation. Meanwhile, T_J is taken with accuracy. Details of the system is described in [3]. A copper VC and a copper plate with the same dimensions of 90 mm × 60 mm × 0.4 mm were used as the testing samples.

A higher duty cycle of laser heating is preferred for minimized perturbation from the off time. For a cycle time Λ of 1 s, the laser off time is set at 50 ms. The corresponding duty cycle χ of the laser heater is 95%. The original T_J curve, T_C curve, and the heat current (power) curve of the vapor chamber and the copper plate samples in the final 60th cycle are shown in Fig. 2. The initial fake T_J temperature with interference is higher than 100 °C, but it decreases very fast after the heating (the laser beam) is shut off because of the fast response of the IR pyrometer. The temperatures should be taken at a delay time after the heat current is shut off and the fake signal has discharged sufficiently. The copper plate sample, with predictable thermal properties, is used as the calibration sample. In this way the delay time is set at 20 ms.

3. Theoretical Grounds of Calibration

The temperature, T_J, at the heating position on the evaporator of the thin vapor chamber in contact with the heater (the semiconductor chip), is an important performance parameter. The infra-red pyrometer detects the thermal radiation signal from the object for temperature measurement. However, the scattered heat laser light is much stronger than the real thermal radiation signal. The non-contact temperature measurement of T_J is severely affected. To suppress the interference, the output beam of the heating laser is switched off for a short period of time. The temperature, T_J, is taken with accuracy while there is no interference laser light. The heating is on-and-off with a cycle time Λ and a duty cycle χ. The T_J is taken once in each cycle. The heat current (power) functions of the continuous heating (CH) scheme, $H_{CH}(h^0, t)$, and the on-off heating (OOH) scheme, $H_{OOH}(h, t)$, are described as:

$$H_{CH}(h^0, t) = h^0, \text{ for t = 0 to } \Lambda \quad (1)$$

$$H_{OOH}(h, t) = \begin{cases} h \\ 0 \end{cases}, \text{ for t} = \begin{cases} 0 \text{ to } \chi\cdot\Lambda \\ \chi\cdot\Lambda \text{ to } \Lambda \end{cases} \quad (2)$$

where h^0 and h are constant numbers.

Calibration of the heat current of on-off heating is necessary for reducing the difference with the continuous heating scheme.

3.1. Calibration Method by Matching the Heat

The heat matching method matches the heat of the on-off heating scheme of $h = h^{(1)}$ to the continuous heating scheme in a cycle:

$$\int_0^{\Lambda} H_{OOH}(h^{(1)}, t)dt = \int_0^{\Lambda} H_{CH}(h^0, t)dt \quad (3)$$

$$h^{(1)} = \frac{h^0}{\chi} \quad (4)$$

$h^{(1)}$ should be larger than h^0 to compensate for the off time in the on-off heating scheme. For duty cycle of 90% and 95%, $h^{(1)}$ is $1.11 \cdot h^0$ and $1.05 \cdot h^0$, respectively. For a higher duty cycle χ, a smaller perturbation by the off time is expected.

3.2. Calibration Method by Matching the Temperature

The measured temperatures, using the on-off heating scheme, are also related to the device characteristics, the cycle time and the duty cycle, and the delay time for temperature acquisition after the heat power is OFF. The corresponding heat power of the on-off heating scheme may not be as simple as just equating the heat. The temperature matching method matches the device temperature of the on-off heating scheme to the continuous heating scheme. The device under test is considered as a system with the heat current as the input and the temperatures T_J, T_C, and T_X as the output. We assume when one temperature output is matched, the other two temperature outputs are also matched. The temperature matching relation is schematically shown in Fig. 3. T_J is seriously affected by the fake signal, and T_X is relatively insensitive to the heat current input. Both are not suitable for the matching parameter.

Therefore T_C is chosen as the parameter for calibration. The heat power of the on-off heating scheme h is used as the tuning parameter. When $h = h^{(2)}$ for H_{OOH}, T_C is matched:

$$T_C\left(H_{OOH}(h^{(2)}, t)\right) = T_C(H_{CH}(h^0, t)) \tag{5}$$

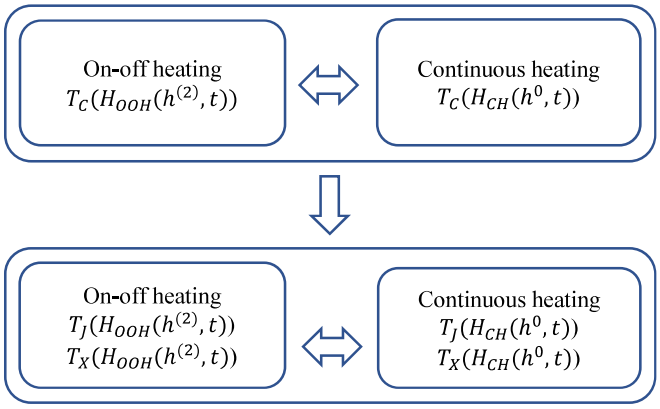

Fig. 3. Calibration procedures of the heat power of on-off heating scheme by matching T_C temperature.

The correction factor γ is the ratio of $h^{(2)}$ of the temperature matching to $h^{(1)}$ of the heat matching:

$$\gamma = \frac{h^{(2)}}{h^{(1)}} = \frac{\chi \cdot h^{(2)}}{h^0} \tag{6}$$

3.3. Effective Heat Capacity of the Vapor Chamber

The vapor chamber is an effective heat spreader so the heater (the semiconductor chip) can be maintained at a lower temperature. The transient response data show a smaller temperature change and a faster heat propagation along the transverse plane to the heat current surge input for the VC compared to the copper plate. The higher surge power, the better temperature stabilization. The vapor chamber showed a peak temperature 9 °C lower than that of the copper plate, to a 1-s 10-W rectangular heat pulse input [3]. The electrical capacitance of an electronic or optoelectronic device is related to its response speed. A high-speed device should have a small capacitance. But a voltage stabilizer circuit requires a large capacitor. It is the same for thermal engineering. The heat source output may not always be a constant. Heat surge can also take place. Here we follow the same concept and use the effective heat capacity C_{eff} for the assessment of temperature stabilization. The effective heat capacity at the T_C position of the device is the variation (functional derivative) of the heat to the temperature:

$$C_{eff} = \frac{\delta Q}{\delta T_C} = \frac{h \cdot dt}{\delta T_C} \tag{7}$$

where δQ is the heat difference, h is the heat current, dt is the time span of the heat current pulse, and δT_C is the temperature difference during dt. The effective heat capacity C_{eff} is more like a system function concept. The heat dissipation of the device is not excluded, whilst for the typical heat capacity measurement the sample is insulated and in a thermal equilibrium state. The heat capacity is inversely proportional to the temperature difference. Using the laser heating source, it is possible to generate the short heat power pulse with a small pulse width dt. The vapor chamber structure is composed of the top and bottom metal plates, the metal wick structure, and the working fluid and the vapor inside the chamber. It is complicated to calculate its heat capacity directly. However, we can estimate the effective thermal capacity of the VC with respect to the copper plate's at the T_C position using Equation (7):

$$\frac{C_{eff}^{VC}}{C_{eff}^{CP}} = \frac{\delta T_C^{CP}}{\delta T_C^{VC}} \tag{8}$$

where δT_C^{VC} and δT_C^{CP} are the temperature differences of the VC and the copper plate, respectively.

4. Experimental Results and Discussion

4.1. Measured T_C Curves

The T_C curves of the VC and the copper plate samples using the continuous heating scheme at the heat current of h^0 and the on-off heating scheme at the heat current of $h^{(1)}$ (the heat match calibration) and $h^{(2)}$ (the temperature match calibration) are shown for comparison in Fig. 4. The duty cycle is 90% in Figs. 4(a) and 4(b), and is 95% in Figs. 4(c) and 4(d). The temperature differences of the VC are smaller than those of the copper plate. The VC is less sensitive than the copper plate for the on-off heating for duty cycle of both 90% and 95%.

4.2 Discussion of the Calibration Methods

The quantitative data of the temperature deviation, ΔT_C between the continuous heating and the on-off heating at $h^{(1)}$ and $h^{(2)}$, for the VC and the copper plate samples, at heat current levels of 3 and 7 W, and duty cycles of 90% and 95% are summarized in Table I. The temperature deviation ΔT_C at $h^{(1)}$ is relatively small 0.5 °C for the VC, and 1.2 °C for the copper plate, at corresponding h^0 of 7 W and 90% duty cycle. At 95% duty cycle, ΔT_C at $h^{(1)}$ is 0.7 °C for the VC, and 1.7 °C for the copper plate. The dependence of ΔT_C on duty cycle is not obvious for the VC. But for the copper plate, 95% duty cycle is better than 90%. ΔT_C of the vapor chamber is less than 1 °C at both $h^{(1)}$ and $h^{(2)}$, and for h^0 from 3 to 7 W. The heat matching calibration method is useful for most applications. If for high accuracy, the temperature matching calibration method can be useful. The dependence of the correction factor γ on the heat current level is also not obvious for the VC.

4.3. Effective Heat Capacity

Measurement of the transient response of a vapor chamber and a copper plate to a 1-s single rectangular heat current pulse was reported in [3]. A pulse heat current with an even shorter width is preferred for achieving a better accuracy using the variation (the functional derivative) method as Equation (7). The heat current function of the on-off heating scheme $H_{OOH}(h, t)$ can be considered as the superposition of a constant value term of 7 W and a periodic ($\Lambda = 1000$ ms) rectangular function $\Pi(t)$ with an amplitude of -7 W (the heat current with a negative amplitude is equivalent to cooling) and a pulse width dt of 50 ms for t = 0 to 1000 ms as:

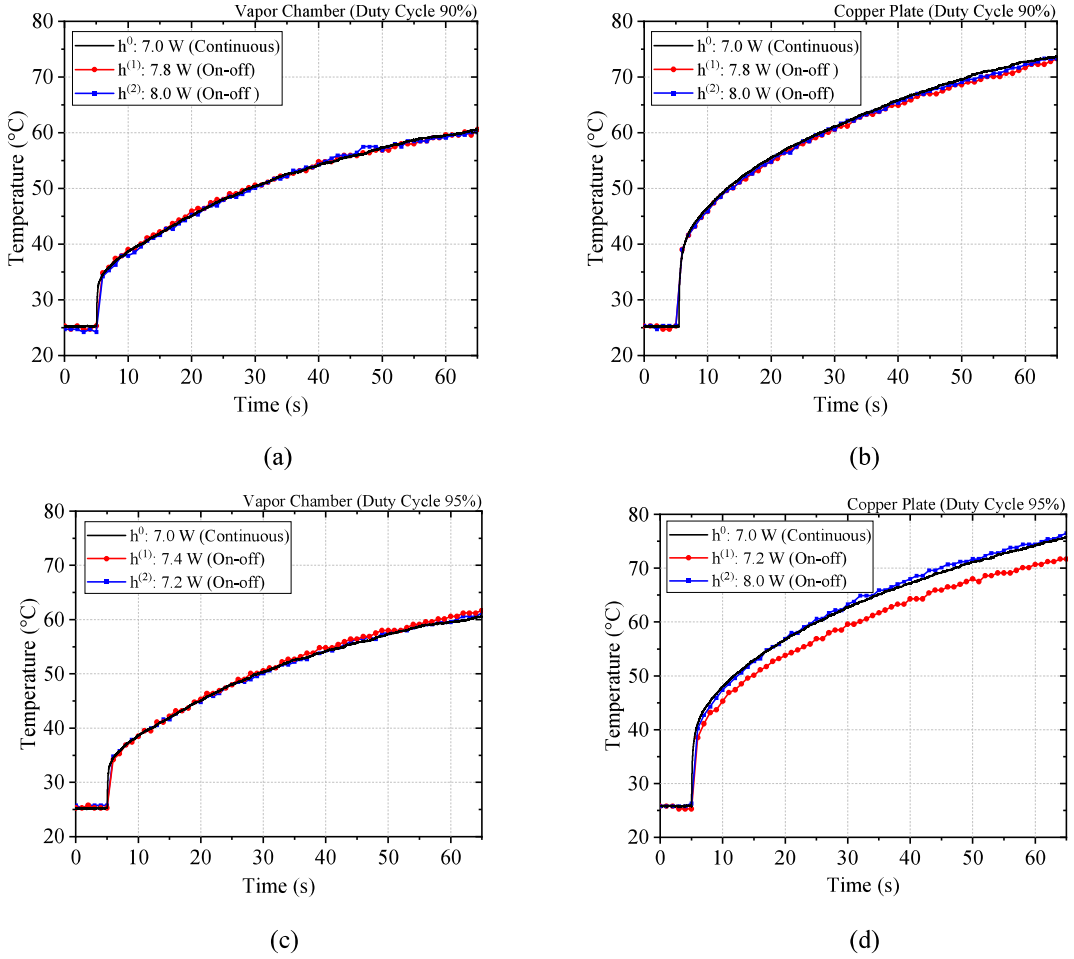

Fig. 4. T_C curves of (a) the VC and (b) the copper plate at 90% duty cycle, and (c) the VC and (d) the copper plate at 95% duty cycle.

TABLE I
RESULTS OF THE TWO CALIBRATION METHODS. $\Delta T_C = T_C(H_{CH}) - T_C(H_{OOH})$.

Parameters	Vapor Chamber				Copper Plate			
χ (duty cycle)	90%		95%		90%		95%	
h^0 (continuous heating)	3.0 W	7.0 W	3.0 W	7.0 W	3.0 W	7.0 W	3.0 W	7.0 W
$h^{(1)}$ (on-off heating)	3.4 W	7.8 W	3.2 W	7.4 W	3.4 W	7.8 W	3.2 W	7.2 W
ΔT_C at $h^{(1)}$	0.6 °C	0.5 °C	0.5 °C	0.7 °C	0.3 °C	1.2 °C	0.2 °C	1.7 °C
$h^{(2)}$ (on-off heating)	3.2 W	8.0 W	3.2 W	7.2 W	3.4 W	8.0 W	3.2 W	8.0 W
ΔT_C at $h^{(2)}$	0.4 °C	0.5 °C	0.5 °C	0.3 °C	0.3 °C	0.7 °C	0.2 °C	0.5 °C
γ (correction factor)	0.94	1.02	1.00	0.97	1.00	1.02	1.00	1.08

$$H_{OOH}(7\text{ W}, t) = 7 - 7 \cdot \Pi\left\{\frac{t-975}{50}\right\}\text{ (W)} \qquad (9)$$

The T_C curve and the heat current curve in the 60th cycle are shown in Figs. 5(a) and 5(b) for the VC and the copper plate, respectively. During the 50-ms heating off time dt, the temperature drop δT_C is -2.1 °C for the VC and -5.3 °C for the copper plate. The temperature drop of the VC is obviously smaller than the copper plate's. This is also consistent with the ΔT_C results of Fig 4. The experiment of applying positive heat pulses of the same conditions to a VC and a copper plate shows similar temperature changes as those in the negative pulse cases. The effective heat capacity of the vapor chamber is 2.5 times larger than that of the copper plate, using Equation (8). The VC utilizing the two-phase mechanism has a larger effective heat spreading area and therefore a larger thermal capacity. For the metal plate utilizing simply the material thermal conductance

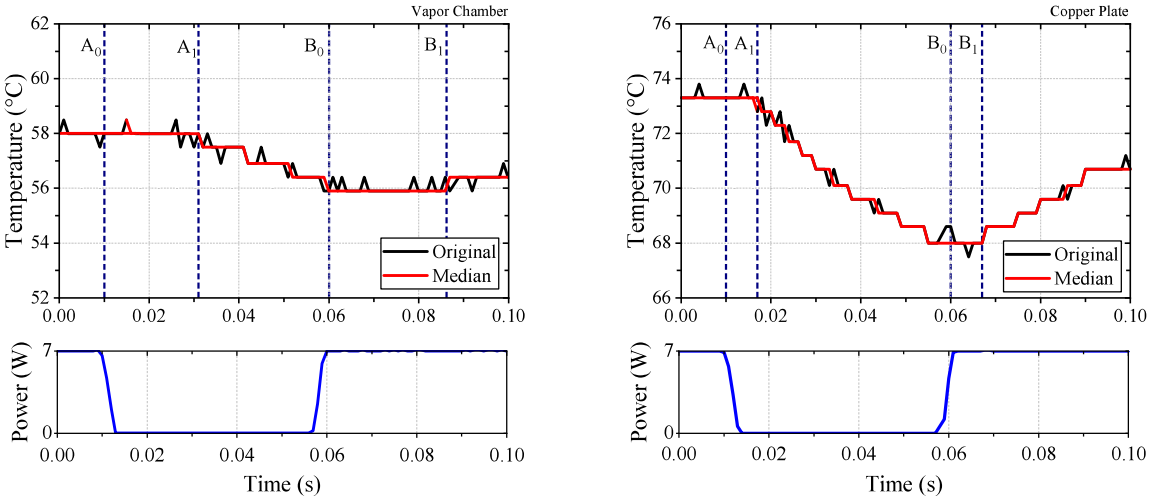

Fig. 5. T_C curve and the heat current curve of (a) the VC, and (b) the copper plate. The heat current is 7 W. The median is used for noise reduction. Thicknesses of the VC and the copper plate are both 0.4 mm.

the temperature gradience in the lateral directions is large so the effective heat spreading area and the capacity are smaller. Therefore, the VC serves as a much better heat spreader and also a temperature stabilizer than the copper plate.

Comparing the turn point of the heat current curve and the turn point of T_C curve as shown in Fig. 5, the delay time of the change of T_C temperature (from A_0 to A_1, and from B_0 to B_1) to respond to the heating on the hot side is estimated. It is 21 to 26 ms for the VC, and but only 7 ms for the copper plate. It is much slower for the T_C temperature to respond to the heating for the VC than the copper plate. The slower response is consistent with the previous conclusion that the vapor chamber has a larger effective heat capacity by comparing the temperature difference as Equation (8). However, the heat spreading in the transverse direction is faster for the VC than the copper plate, as reported in [3]. The thermal convection is faster than the thermal diffusion.

5. Conclusions

Using laser heating and infra-red pyrometer temperature measurement for characterization of thin vapor chambers is accurate and fast for mass production applications, compared with the contact measurement method. Two calibration methods of the performance characterization of the thin vapor chambers by photonics technologies were proposed and the experimental results were discussed. With the calibration, the temperature accuracy was within ±1 °C. The transient response of vapor chamber showed temperature stabilizing. The temperature deviation using pulsed heating from constant heating was not quite significant for the vapor chamber. The effective heat capacity was proposed and used for the assessment of temperature stabilizing transient performance. By analyzing the experimental data during the 50-ms laser off time, the effective heat capacity of the vapor chamber is 2.5 times larger than that of the copper plate.

Acknowledgments

This project was partially supported by Bureau of Energy, Ministry of Economic Affairs, Taiwan (ROC) under grant 111-D0706.

References

1. G. Patankar, *et al.*, "A method for thermal performance characterization of ultrathin vapor chambers cooled by natural convection," *Journal of Electronic Packaging*, vol. **138**, 010903, 2016.
2. X. Jiang, *et al.*, "A non-contact thermal testing system for ultra-thin vapor chamber," *Review of Scientific Instruments*, vol. **92**, 124902, 2021.
3. K. Y. Hsu, *et al.*, "A Thermal Performance Characterization Method for Thin Vapor Chambers by Photonics Technologies," *2024 40th Semiconductor Thermal Measurement, Modeling & Management Symposium (SEMI-THERM)*, San Jose, CA, USA, pp. 76-82. https://ieeexplore.ieee.org/document/10535014